Digital Implementation of Reference Current Generation Schemes for Current Error Space Phasor Hysteresis Controller based Shunt Active Power Filters

Siddharthsinh K. Chauhan
Department of Electrical Engineering,
Institute of Technology,
Nirma University, Ahmedabad,
Gujarat, India.
siddharthsinh2007@gmail.com

Mihir C. Shah
Department of Electrical Engineering,
Institute of Technology,
Nirma University, Ahmedabad,
Gujarat, India.
mihir_1104@yahoo.com

P. N. Tekwani
Department of Electrical Engineering,
Institute of Technology,
Nirma University, Ahmedabad,
Gujarat, India.
pn.tekwani@nirmauni.ac.in

***Abstract* – Power quality improvement devices like Shunt Active Power Filters (SAPF) are commonly employed to reduce harmonics introduced by Non-linear loads. Performance of SAPF using current error space phasor based hysteresis controller is presented in this paper to prove controller's versatile nature. Dynamic behavior of the SAPF is demonstrated for changes in load. Comparative study for Digital Signal Processor (DSP) based implementation of Instantaneous Reactive Power Theory (IRP) and Fryze current computation method for generation of reference compensating currents is presented in this paper. Experimental results for different strategies of reference compensating currents generated using DSP TMS320LF2407A are demonstrated in the present work. The controller switches voltage vectors adjacent to the voltage vector at the point of common coupling and hence keeps the current error within desired hexagonal boundary during steady state as well as transient operating conditions. The effectiveness of the proposed controller is demonstrated by simulation studies.**

Keywords - Active Power Filters, Current Error Space Phasor, DSP, Fryze Current Computation Technique, Instantaneous Reactive Power Theory, Self Adaptive Hysteresis Controller

I. INTRODUCTION

Nonlinear loads draw non-sinusoidal unbalanced currents from ac mains resulting in harmonic injection, reactive power burden, excessive neutral currents and unbalanced loading of ac mains. These harmonics interfere with sensitive electronic equipment and cause unnecessary losses in electrical machinery. Conventionally, passive filters consisting of tuned L-C filters have been broadly used to suppress harmonics because of low initial cost and high efficiency. However, passive filters have many disadvantages, such as large size, parallel and series resonance that could be created with both load and utility impedances, filtering characteristics strongly affected consequently by the source impedance [1].

Shunt active filters were initially proposed in 1971 by Sasaki and Machida [2] as a means of removing current harmonics. When the Active Power Filter (APF) is connected in parallel with the harmonic load, it is called shunt APF [3]. The shunt APF operates as a current source that injects a compensating current in order to cancel the harmonic currents and the reactive fundamental current generally produced by nonlinear non-resistive loads. The shunt APF is thus suitable for nonlinear loads which introduce current harmonics, while for nonlinear loads that produce voltage harmonics, a series APF is used [4]. Application of filter is not only limited to harmonic compensation but it is also used for harmonic damping, harmonic isolation, harmonic termination, reactive-power control for power factor correction and voltage regulation, load balancing, voltage-flicker reduction, and/or their combinations. Many approaches such as notch filter [5], instantaneous reactive power theory [6], synchronous detection method [7], synchronous d–q frame method [8], flux based control [9] and closed-loop PI controllers [8-9], and sliding mode control [10-11] are used to improve the performance of the APFs. These approaches have become feasible because of the advent of new microelectronic devices such as Digital Signal Processors (DSPs) and availability of fast and accurate Hall effect sensors.

This paper presents the performance of 3-Φ SAPF using the Instantaneous Reactive Power (IRP) theory and Fryze current computation technique. Both the control strategies are rigorously simulated for the reference current generation. Current error space phasor based fixed band hysteresis controller is used to implement the SAPF. Experimental results of both the control strategies are presented using DSP TMS320LF2407. Paper mainly focuses on the implementation considerations of both the control strategies in the DSP. It is systematically evaluated that Fryze current computation technique is easier to implement and better resolution can be obtained in the calculations to achieve the reference compensating currents than obtaining the same with IRP theory with the same DSP. Also the behavior of SAPF for load variations is studied in the paper.

II. SHUNT ACTIVE POWER FILTER

The shunt active power filter operates as a current source injecting the harmonic components generated by the load but phase shifted by 180^0. The current compensation characteristic of the shunt active power filter is shown in Fig 1.

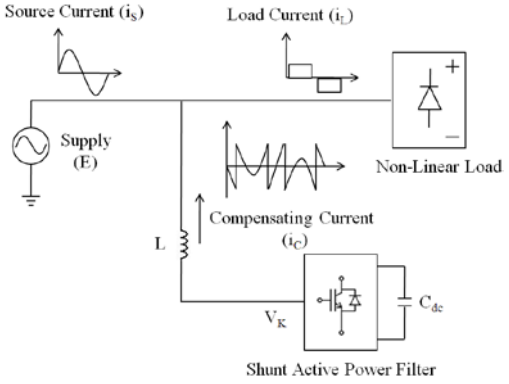

Fig. 1 Shunt active power filter

III. PRINCIPLE OF SPACE PHASOR BASED CURRENT HYSTERESIS CONTROLLER

The space phasor of the APF current (i_c) and voltage (V_k) as well as the voltage at the point of common coupling (PCC) (E) are respectively given by:

$$i_c = \frac{2}{3}*(i_{ca} + a i_{cb} + a^2 i_{cc}) \quad (1)$$

$$V_k = \frac{2}{3}*(V_a + aV_b + a^2 V_c) \quad (2)$$

$$E = \frac{2}{3}*(E_a + aE_b + a^2 E_c) \quad (3)$$

Where,

$$a = e^{j\frac{2\pi}{3}}$$

Now, rate of change of compensating current is

$$\frac{di_c}{dt} = \frac{1}{L}(V_k - E)$$

Where, L = APF inductor

Now current error space phasor is

$$\Delta i = i_c - i_c^* \quad (4)$$

Where i_c^* is reference current space phasor.

Thus rate of change of current error is

$$L\frac{d\Delta i}{dt} = (V_k - E) - L\frac{di_c^*}{dt} \quad (5)$$

In order to eliminate the current error Δi, the desired output voltage vector V_o^* is obtained from (5) as

$$V_0^* = E + L\frac{di_c^*}{dt} \quad (6)$$

The direction at which the current error space phasor moves is given by

$$\frac{d\Delta i}{dt} = \frac{V_k - V_0^*}{L} \quad (7)$$

Different strategies have been proposed to choose the desired inverter voltage vector to keep the current error space phasor within the boundary [15-20]. The derivative $d\Delta i/dt$ has a vital role in diminishing the number of switching. Choosing a voltage vector V_k, which results in a minimum value of $d\Delta i/dt$ is a necessity to accomplish this task. For the conventional hysteresis current controller (HCC) technique, the coordination of the switching does not exist; however, SVM technique causes reduced switching. On the other hand, the utilization of nonzero vectors instead of the zero vector gives steep slope for the current error due to large voltage difference V_o^*-V_k. Thus, a set of space vectors, two vectors plus the zero vector, is to be applied depending on the position of the desired space voltage vector V_o^*.

IV. PROPOSED CURRENT ERROR SPACE PHASOR BASED HYSTERESIS CONTROLLER

In the present hysteresis controller, the current error space phasor is kept within a boundary, by applying one of the three inverter voltage vectors which are adjacent to the voltage vector V_o^* so that deviation of current error space phasor is minimum. Fig. 2 shows the inverter voltage vectors and direction of current error space phasor movement for two positions of desired output space voltage vector V_o^*. This set of directions can be used to define a boundary for the error space phasor, beyond which it should not be allowed to move. For example if the error space phasor moves in a direction parallel to any direction bounded by the directions of OA and OF, it can touch a boundary XZ as shown in Fig. 3(a).This boundary can be decided to be anywhere at a distance 'h' along the j_C axis. Similarly, the directions OC and OB define another boundary YX along the j_A axis and the directions OD and OE define the third boundary along the j_B axis. The same triangular boundary exists for all the odd sectors. In the same manner triangular boundary shown in Fig. 3(b) exists for all the even sectors. Fig. 4 shows the boundary within which the error space phasor can move when V_o^* moves through all the sectors.

A. Inverter Voltage Selection

This hysteresis controller uses only vectors which are adjacent to V_o^*. The proposed controller divides the triangular boundary to three regions and each of these regions is associated with a suitable inverter voltage vector (depending on the sector) which will take the error space phasor towards the opposite side of the triangular boundary. The triangular boundary for odd sectors is divided in to three regions R_1, R_2 and R_3, while that for even sectors is divided into $\overline{R_1}$, $\overline{R_2}$ and $\overline{R_3}$ as shown in Fig. 4 (a) and (b), respectively. When the current error space phasor hits anywhere in a particular region, a voltage vector is selected so that the current error space phasor moves towards the opposite side. For odd sectors the boundaries are placed along the j_A, j_B, j_C axes and for even sectors the boundaries are placed along the $-j_A$, $-j_B$, $-j_C$ axes and this would result in the combined boundary as shown in Fig. 5(a). Now, for this triangular boundary, the error space phasor moves to double the distance, along the $-j_A$, $-j_B$, $-j_C$ axes in the case of odd sectors and along j_A, j_B, j_C axes for the even sectors. If boundaries are placed along all these axes, for both odd as well as even sectors, it would result in a hexagonal boundary as shown in Fig. 5(b). The different regions and respective inverter voltage vectors to be switched are shown in Table I.

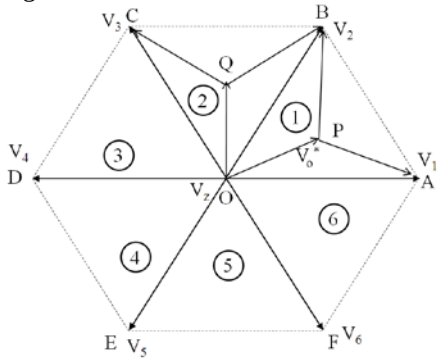

Fig. 2 Output space voltage vector and direction of current error space phasor

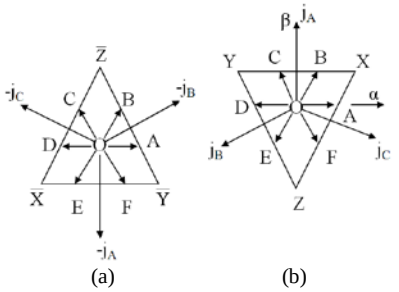

(a) (b)

Fig. 3 Boundary of Δi (a) in Sector-2, (b) in Sector-1

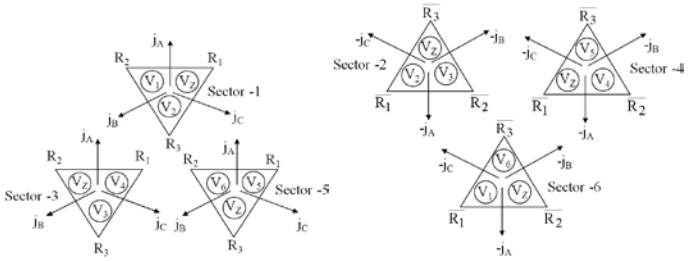

(a) (b)

Fig. 4 Regions and corresponding voltage vectors for (a) odd sectors (b) even sectors

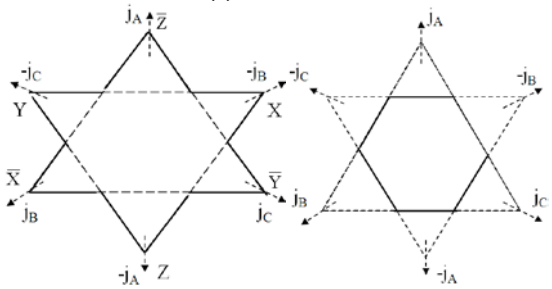

Fig. 5 (a) Boundary of Δi (initial) (b) Boundary of Δi (modified)

TABLE I
VOLTAGE VECTORS TO BE SWITCHED FOR VARIOUS REGIONS

	Regions					
Sector	R_1	R_2	R_3	$\overline{R_1}$	$\overline{R_2}$	$\overline{R_3}$
1	V_Z	V_1	V_2	-	-	-
2	-	-	-	V_2	V_3	V_Z
3	V_4	V_Z	V_3	-	-	-
4	-	-	-	V_Z	V_4	V_5
5	V_5	V_6	V_Z	-	-	-
6	-	-	-	V_1	V_Z	V_6

B. Sector Selection Logic

The proposed hysteresis controller uses a self-adapting logic to identify the instants at which the V_o^* crosses from one sector to another. This sector change is identified with the help of another set of comparators placed a little further than the comparators used for the vector selection. Fig. 6 shows the outer hysteresis band placed along all the axes and direction along which sector change takes place.

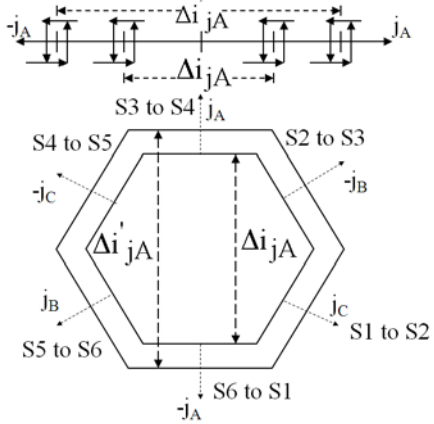

Fig. 6 The outer hysteresis band and the sector changeovers

V. REFERENCE COMPENSATING CURRENT CALCULATION

The shunt active power filter shown in Fig. 1 consists of six semiconductor power switches, a dc-link capacitor as a voltage source and three reactors for limiting the current rate of rise

A. Instantaneous Reactive Power Theory

Instantaneous reactive power theory is explained by the block diagram shown in Fig. 7 [6], [21]. The compensated currents are calculated as follows:

$$i_{c\alpha}^{*} = \frac{E_\alpha (p_{ac} + p_{loss}) - E_\beta q}{E_\alpha^{\,2} + E_\beta^{\,2}} \tag{8}$$

$$i_{c\beta}^{*} = \frac{E_\alpha q + E_\beta (p_{ac} + p_{loss})}{E_\alpha^{\,2} + E_\beta^{\,2}} \tag{9}$$

Where,
$i_{c\alpha}^{*}$, $i_{c\beta}^{*}$ = Reference compensating currents along α and β axis.
p_{ac} = ac component of active and reactive power
P_{loss} = Switching losses of the inverter
q= reactive power
E_α, E_β = Supply voltage along α and β axis
Therefore compensating currents in three phase form are

$$i_{ca}^{*} = \sqrt{\frac{2}{3}} i_{c\alpha}^{*} \tag{10}$$

$$i_{cb}^{*} = \sqrt{\frac{1}{6}} i_{c\alpha}^{*} + \sqrt{\frac{1}{2}} i_{c\beta}^{*} \tag{11}$$

$$i_{cc}^{*} = -\sqrt{\frac{1}{6}} i_{c\alpha}^{*} - \sqrt{\frac{1}{2}} i_{c\beta}^{*} \tag{12}$$

Where,
i_{ca}, i_{cb}, i_{cc} = Compensating currents of a,b,c phase
i_{ca}^{*}, i_{cb}^{*}, i_{cc}^{*} = Reference Compensating currents of a,b,c phase.

B. Fryze Current Computation Technique

The generalized Fryze current method presents a minimum rms value so that the same three phase average active power is drawn from the source as the original load current shown in Fig. 8. This reduces the ohmic losses in the transmission line and guarantees linearity between the supply voltage and compensated current [22]. The average conductance (G_e) passing through Butterworth design based Low Pass Filter (LPF). The desired reference source currents calculated from the active current, after compensation, can be written as,

$$i_{ca}^{*} = i_{la} - i_{wa} \tag{13}$$

$$i_{cb}^{*} = i_{lb} - i_{wb} \tag{14}$$

$$i_{cc}^{*} = i_{lc} - i_{wc} \tag{15}$$

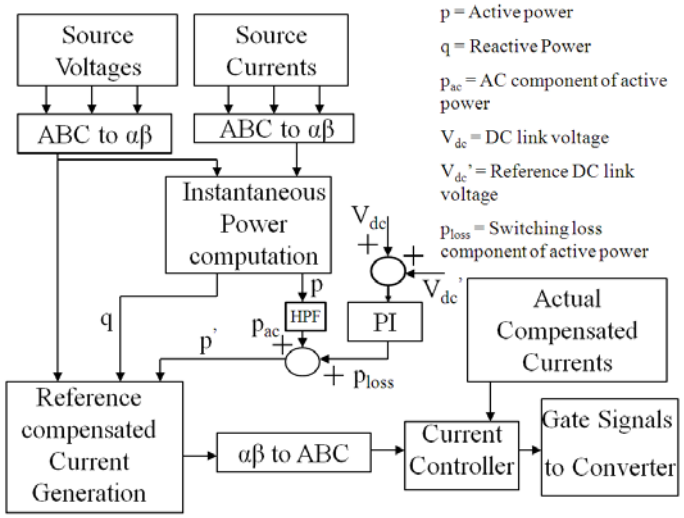

Fig. 7 Control scheme for Instantaneous Reactive Power Theory

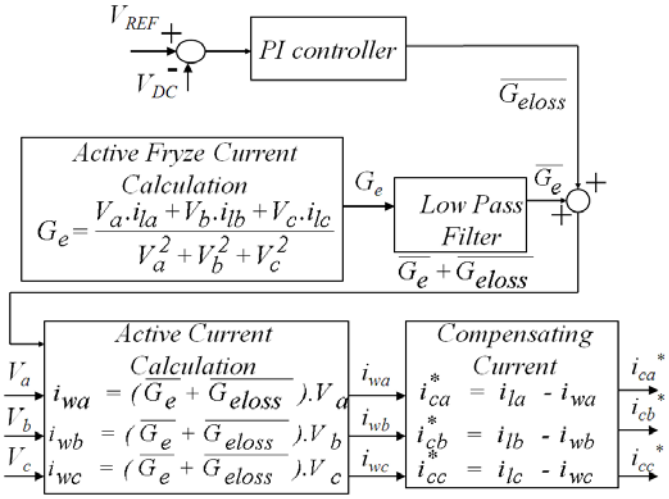

Fig. 8 Control scheme for Fryze current computation technique

VI. IMPLEMENTATION CONSIDERATIONS

A. Signal Conditioning

The current and voltage signals are sensed using the Hall effect sensors and instrumentation amplifiers. This acquisition system is built to reduce the amplitude of the signal reference in the range of 0 – 3.3 V and the output signals have the additional characteristic of a low output impedance with the objective of wasting as much as less time in the Analog to Digital Conversion.

B. Control Strategies: Practical Implementations.

The control strategies i.e. the instantaneous reactive power theory and the fryze current computation technique are being carried out using TMS320LF2407A. The control strategies that are explained in the earlier sections have some differences in implementation using DSP. Table II shows the comparison of implementation considerations of shunt active power filter.

TABLE II
COMPARISON OF BOTH STATEGIES

Parameter	*IRP*	*Fryze*
Dynamic Response	Good	Poor
Linearity	Poor	Better
Execution time in DSP 2407.	6μs (approx)	3.5μs (approx)
Axis transformation (3ϕ-2ϕ)	Required	Not required
Zero sequence components	Not affected	Affected
Power Definitions	$\alpha\beta$ axis	*abc* axis
Resolution of bits in DSP 2407.	Poor	Better

VII. SIMULATION RESULTS

The space phasor based current hysteresis controlled shunt active power filter is simulated using Matlab7.5. Various simulation results are obtained under ideal mains voltage conditions. The essential parameters selected for simulation studies are: fundamental frequency = 50 Hz, rectifier load inductance = 1mH, rectifier load resistance = 50 Ω, 3-Φ (Line-Neutral) ac supply voltage = 230 V, Dc link voltage V_{dc} = 600 V, APF side inductance = 1mH. Fig. 9(a) and Fig. 9(b) shows the sectors of the hexagonal boundary where in V_o^* lies at particular instant and corresponding vectors switched.

A. Instantaneous Reactive Power Theory

Simulation is carried out using generalized instantaneous reactive power theory. Results are shown in Fig. 10(a) and Fig. 10(b). This active power filter helps to reduce the source current THD from 28.56 % (without compensation) to 9.59 %. Results of Fig. 10(a) clearly depict that controller is fast and accurate enough to enable actual compensating current to track the reference compensating current. Current error space phasor plot is shown in Fig. 10(b). It is seen that current error is restricted well within the hexagonal boundary. Sector change is also clearly visible. Hence the active power filter is able to compensate for any type of change in system. Fig. 10(c) shows the response of SAPF when load is changed. Results prove that the active power filter can be used in actual system where load change occurs rapidly.

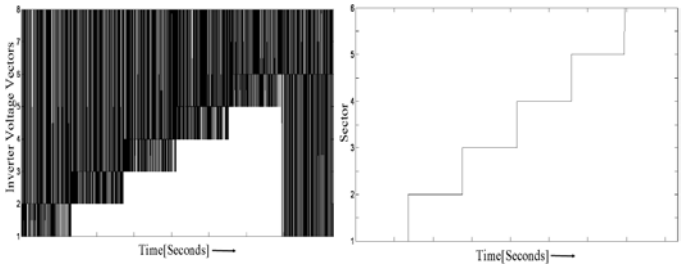

(a) (b)

Fig. 9(a) Inverter voltage vector switched for various sectors (b) Sectors of voltage space phasor structure

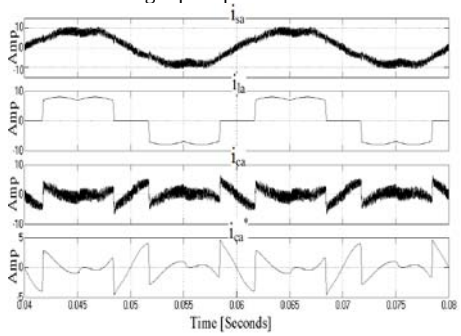

Fig. 10 (a) Instantaneous reactive power theory results for phase A: source current (i_{sa}), load current (i_{la}), actual compensating current (i_{ca}), reference compensating current (i_{ca}*)

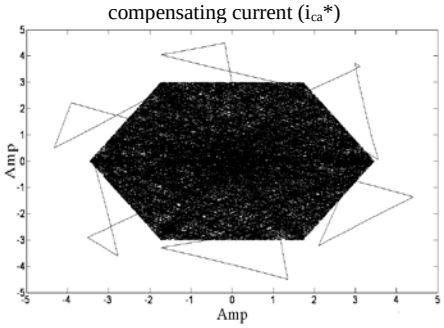

Fig. 10(b) Current error space phasor [X-axis: 1A/div; Y-axis: 1A/div]

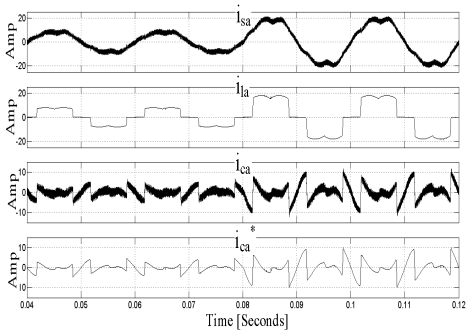

Fig. 10(c) Instantaneous reactive power theory results for phase A

B. Fryze Current Computation Technique.

This method for active power filter helps to reduce the source current THD from 28.56 % (without compensation) to 6.38 %. Results are given in Fig. 11(a) and Fig. 11(b). This method is easy to implement. Results clearly depict that controller is fast and accurate enough to track actual compensating current in accordance with reference compensating current. Current error space phasor plot is shown in Fig. 11(b). It is seen that current error is restricted well within the hexagonal boundary. Sector change is also clearly visible. Fig. 11(c) shows the response of SAPF when load is changed. Results prove that the active power filter can be used in actual system where load change occurs rapidly. Performance of Shunt Active Power filter is shown in table V for different schemes of reference compensating current generation.

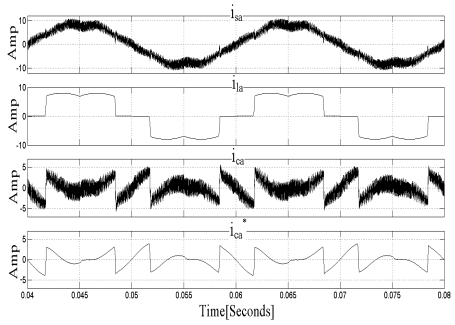

Fig. 11(a) Fryze Current Computation Technique results for phase A: source current (i_{sa}), load current (i_{la}), actual compensating current (i_{ca}), reference compensating current (i_{ca}*)

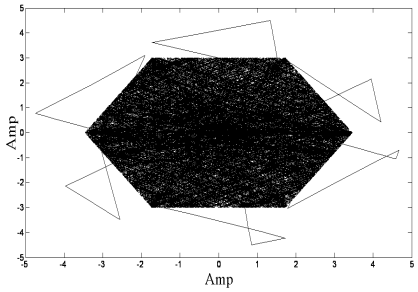

Fig. 11(b) Current error space phasor [X-axis: 1A/div; Y-axis: 1A/div]

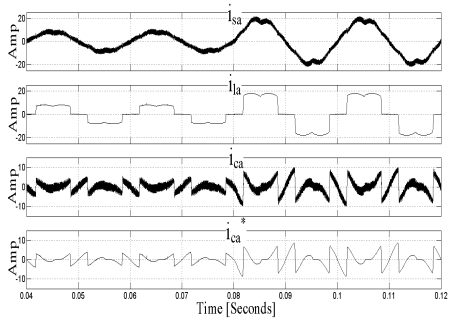

Fig. 11(c) Fryze Current Computation Technique results for phase A

TABLE V
PERFORMANCE OF SHUNT ACTIVE POWER FILTER

Refernce current generation schemes	*Without using SAPF (THD %)*	*SAPF using controller With outer Hysteresis band (THD %)*
IRP	28.56	9.59
Fryze		6.38

C. Unbalanced Supply Mains

Performance of the active power filter is studied for unbalanced supply conditions Here a-phase voltage (Line-Neutral) is kept 207 V while b & c phase (Line-Neutral) voltage is kept 230 V. Results of Fig. 12(a) and 12(b) indicate that proposed active power filter compensates the load harmonics satisfactory even under unbalanced supply mains conditions.

D. Effect of reference compensating current generation methods on switching frequency

Fig. 13(a), 13(b), 14(a) and 14(b) shows the plot of inverter output line voltage and it's FFT for IRP theory and Fryze current computation methods respectively. Results indicate that switching frequency variation (18 kHz – 22 kHz) remains same for both reference compensating current generation schemes. Thus, it is the hysteresis band, filter inductance and dc-link capacitance of inverter which affects the switching frequency.

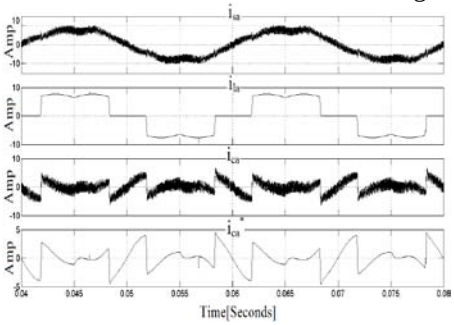

Fig. 12 (a) IRP theory results for unbalanced supply mains: phase A

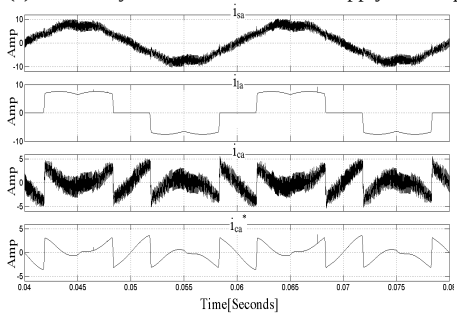

Fig. 12(b) Fryze Technique results for unbalanced supply mains: phase A

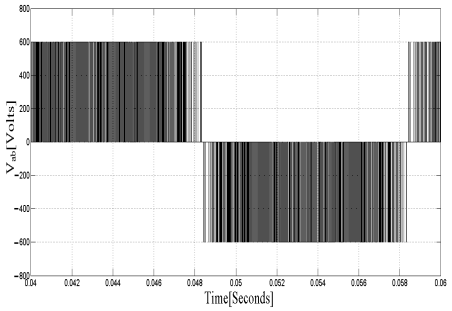

Fig. 13 (a) IRP theory results for Inverter output voltage V_{ab}

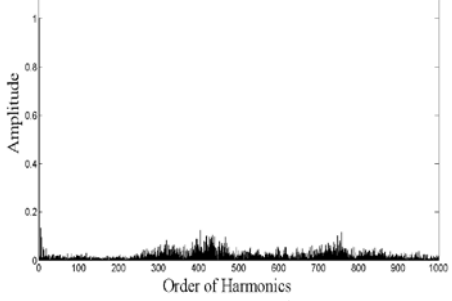

Fig. 13 (b) IRP theory: normalized FFT of Inverter output voltage V_{ab}

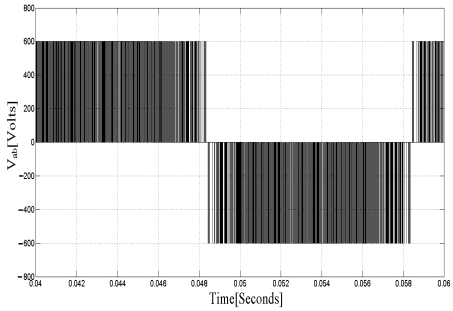

Fig. 14 (a) Fryze Technique results for Inverter output voltage V_{ab}

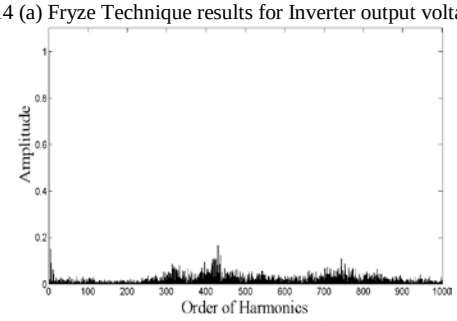

Fig. 14 (b) Fryze Technique: normalized FFT of Inverter output voltage V_{ab}

VIII. EXPERIMENTAL RESULTS

To validate the performance, a prototype test bed has been built for 415V, three phase utility. The whole control algorithm being implemented using DSP TMS320LF2407A. The load is emulated by a three phase diode bridge rectifier with a resistance of 100Ω and a smoothing capacitor. Fig 15 (a) and (b) show the source current of SAPF obtained by subtracting load current with the compensating currents in digital storage oscilloscope for both the methods, respectively.

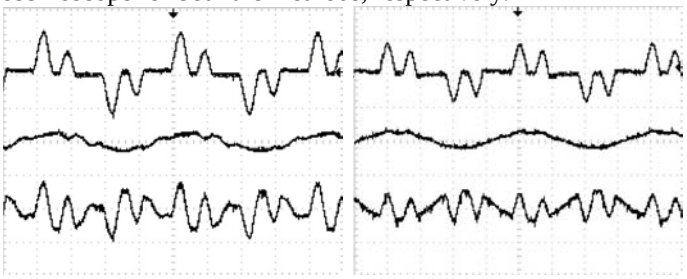

(a) (b)

Fig. 15: Upper Trace: i_{la} , Middle Trace: i_{sa} , Lower Trace : i_{ca*}
[Scale : X axis: 5ms, Y axis: 2A/div], (a) IRP, (b) Fryze computation

IX. CONCLUSION

A unique approach of applying space phasor based current error hysteresis controller to shunt active power filter is presented in this paper. Performance of the controller is tested for steady state as well as for changes in load with two different methods of reference compensating current generation applied to shunt active power filter. Results prove the versatile nature of the controller which can be used for any type of reference compensating current generation technique and can handle rapid load changes. APF compensates properly even for unbalanced supply mains conditions. It is established that reference compensating current scheme has no effect on switching frequency of inverter. Comparison for DSP TMS320LF2407A based implementation of IRP theory and Fryze current computation method for generation of reference compensating currents is shown in the paper. Experimental results of reference current compensating currents for both methods are presented and are proper in nature. The simulation studies show that response of controller is good and is able to maintain the current error within desirable hexagonal boundary. The APF is able to compensate the harmonics as a result of which line current is having low %THD. Harmonic compensation is better with Fryze current computation technique compared to IRP technique.

X. REFERENCES

[1] H. Akagi, New Trends in Active Filters for Power Conditioning, *IEEE Transactions on Industry Applications, Vol. 32*(Issue 6): pp. *1312–1322, Nov.-Dec. 1994.*

[2] H. Sasaki and T. Machida, A New Method to Eliminate AC Harmonic Currents by Magnetic Flux Compensation, *IEEE Trans. Power Appl. Syst., Vol. PAS-90*, (Issue 5): pp. 2009-2019,*1971*.

[3] B. Singh, K. Al-Haddad and A. Chandra, A Review of Active Filters for Power Quality Improvement , *IEEE Transactions on Industrial Electronics, Vol. 46*, (Issue 5): pp. *960–971, Oct. 1999.*

[4] Z. Wang, Q. Wang, W. Yao and J. Liu, A Series Active Power Filter Adopting Hybrid Control Approach, *IEEE Trans. on Power Electronics, Volume 16*(Issue 3): pp. *301-310, May 2001.*

[5] G. Kamath, N. Mohan, V.D. Albertson, Hardware implementation of a novel reduced rating active filter for threephase, four-wire loads, *IEEE-APEC Conf*., pp. 984–989, 1995.

[6] T. Furuhashi, S. Okuma, Y. Uchikawa, A study on the theory of instantaneous reactive power , *IEEE Trans. On Ind. Electron Vol. 37*(Issue 1): pp. *86–90, 1990*.

[7] C.L. Chen, C.E. Lin, C.L. Huang, An active filter for unbalanced three-phase system using synchronous detection method, *IEEE-PESC Conf., pp. 1451–1455, 1994.*

[8] S. Bhattachrya, D. Divan, Synchronous Frame based controller implementation for a hybrid series active filter systems, *IEEEIAS Annual Meeting, pp. 2531–2540, 1995.*

[9] S. Bhattacharya, A. Veltman, D.M. Divan, R.D. Lorenz, Flux based active filter controller, *IEEE-IAS Annual Meeting, pp. 2483–2491, 1995.*

[10] Z. Radulovic, A. Sabanovic, Active filter control using a sliding mode approach, *IEEE-PESC Conf. , pp. 177–182, 1994.*

[11] S. Saetieo, R. Devaraj, D.A. Torrey, The design and implementation of a three-phase active power filter based on sliding mode control, *IEEE Trans. Ind. Appl. vol. 31*,(Issue 5): pp. *993–1000, 1995.*

[12] M.P.Kazamierkowski, W.sulkowski and M.A.Dzieniokowski , Novel space vector based current controllers for PWM inverters, *IEEE Transactions on Power Electronics, Vol.6*, (Issue 1): pp. *158-166, January 1991.*

[13] C.T.Pan and T.Y.Chang, An improved hysteresis current controller for reducing switching frequency, *IEEE Transactions on Power Electronics, Vol.9*, (Issue 1): pp. *97-104, 1994.*

[14] T.Y.Chang, K.L.Lo and C.T.Pan, A novel vector control hysteresis current controller for induction motor drives, *IEEE Transactions on Energy conversion, Vol.9* (Issue 2), *June 1994.*

[15] B. H. Kwon, T. W. Kim and J. H. Youm, Novel SVM based hysteresis current controller, *IEEE Transactions on Power. Electronics, Vol.13*, (Issue 2): pp. *297-307, March 1998.*

[16] Baiju, M.R., Mohapatra, K.K., Kanchan, R.S., Tekwani, P.N., and Gopakumar, K., A space phasor based self adaptive current hysteresis controller using adjacent inverter voltage vectors with smooth transition to six step operation for a three phase voltage source inverter, *EPE Journal, Vol. 15* (Issue 1): pp. *36–47,2005.*

[17] Tekwani, P.N., Kanchan, R.S. and Gopakumar, K., Current-error space-vector-based hysteresis PWM controller for three-level voltage source inverter fed drives, *IEE Proeedings on Electr. Power Appl., Vol. 152*, (Issue 5): pp. 1283-1295, *September 2005.*

[18] Chauhan, S.K., Shah, M.C., Tekwani, P.N., Current Error Space Phasor Based Fixed Band Hysteresis Controller Employed for Shunt Active Power Filter, *NUICONE Conf.,2010.*

[19] Chauhan, S.K., Shah, M.C., Tekwani, P.N., Implementation Considerations of Shunt Active Power Filter using DSP for Two Different Strategies of Reference Current Generation, *ICISET, Vol.1, pp. 306-311,2011.*

[20] Tekwani, P.N., Chauhan, S.K., Performance of space phasor based current controller with various schemes for reference current generation for shunt active power filter, *NUCONE Conf., 2009.*

[21] S. Bhattachrya, D. Divan, Synchronous Frame based controller implementation for a hybrid series active filter systems, *IEEEIAS Annual Meeting, pp. 2531–2540, 1995*.

[22] H.Akagi, Edson hirokazu watanabe and Mauricio Aredes, Instantaneous Reactive power theory and applications to Power Conditioning (IEEE press, 2007, pp. 96-147).